Springer
Acta Mechanica Sinica
CrossMark click for updates

• RESEARCH PAPER •

Acta Mech. Sin., Vol. 41, 424604 (2025)
https://doi.org/10.1007/s10409-024-24604-x

# How does the shape of an inclusion near a bi-material interface evolve to maintain uniform internal stress: the anti-plane shear case

Ming Dai*, and Cun-Fa Gao

*State Key Laboratory of Mechanics and Control for Aerospace Structures, Nanjing University of Aeronautics and Astronautics, Nanjing 210016, China*

Received September 30, 2024; accepted October 18, 2024; published online March 12, 2025

In the theory of two-dimensional linear elasticity, an elliptical inclusion is known to attain a constant stress field when perfectly buried in an infinite homogeneous matrix if a uniform eigenstrain is applied to it. The focus of this paper falls on the question: when the initially elliptical inclusion verges on a bi-material interface, what would happen to its configuration if it is required to retain the internal constant stress? Specifically, we explore the anti-plane shear version of this question (the version of plane deformations or three-dimensional deformations seems, however, insoluble at this stage), in which an inclusion undergoing a uniform (anti-plane shear) eigenstrain is embedded in a bi-material structure composed of two infinite elastic half-planes whose interface is straight and perfectly bonded, and the shape of the inclusion is to be determined such that the eigenstrain-induced stress inside the inclusion appears to be a constant. Unlike most optimization methods-driven solution procedures for finding the shape of the inclusion approximately in which huge computation is required, we derive by a rigorous theoretical analysis an exact integral equation with respect to the boundary curve of the inclusion that is sufficiently and necessarily related to the existence of a constant stress inside the inclusion. We solve this integral equation via the use of some analytic techniques and present in several illustrative examples a variety of shapes of the inclusion achieving constant stresses. We discover some interesting phenomena for the evolution of the shape of the uniformly stressed inclusion relative to the stiffness of the nearby interface.

**Bi-material interface, Uniform stress, Eshelby conjecture, Half-plane, Inverse problem**

**Citation:** M. Dai, and C.-F. Gao, How does the shape of an inclusion near a bi-material interface evolve to maintain uniform internal stress: the anti-plane shear case, Acta Mech. Sin. 41, 424604 (2025), https://doi.org/10.1007/s10409-024-24604-x

## 1. Introduction

The elasticity theory of inclusions surrounded by a foreign matrix plays an essential role in the mechanical modelling [1-4] and mathematical analysis [5-7] of particle-filled composites. One of the fundamental problems in this research area is concerned with the macroscopic response of the composite inclusion-matrix system to external loadings, and therefore focuses on optimal bounds of the overall properties of the composite system for a given volume fraction of the inclusions. Obviously, the overall properties of the composite system are strongly related to the corresponding microstructure, i.e., the configuration and arrangement of the inclusions. It has been shown by Liu [8] and Silvestre [9] that extremal overall properties of the composite system correspond to special configurations of the inclusions requiring that a constant stress/strain is achieved inside each inclusion for certain external loadings imposed on the composite system. Consequently, the problem of the uniformity of the stress in inclusions is essentially associated with the design of extremal particulate composites. On the other hand, it was shown in Ref. [10] that the shape of inclusions holding uniform stress minimizes the stress concentration in the entire composite,

*Corresponding author. E-mail address: mdai@nuaa.edu.cn; m.dai@foxmail.com (Ming Dai)
Executive Editor: Zishun Liu

leading to an increase in the strength of the composite. Additionally, the problems of inclusions with uniform stress are found to have direct links with a broad class of energy minimization problems in multiphase composites [11]. We particularly mention that the problem of the uniformity of the stress within inclusions is closely related to (sometimes equivalent to) two specific kinds of inverse problems of holes embedded in an elastic solid, i.e., the design of equally strong holes [12-14] and that of harmonic holes [15,16].

One of the classical results established in two-dimensional linearly elastic deformations of either plane strain/stress or anti-plane shear states that an isolated elliptical inclusion enveloped by an infinite elastic matrix could acquire a constant internal stress field if the loading applied to the matrix remotely is uniform or the eigenstrain exerted on the inclusion is uniform [17,18], and any isolated non-elliptical inclusion cannot share this property of constant stress [19,20]. Similar results of an isolated ellipsoidal inclusion in three-dimensional linear isotropic elasticity were identified by Eshelby [21], and the related uniqueness of the ellipsoidal shape was verified (except for the strong version) by Liu [22], Kang and Milton [23], Ammari et al. [24] and Yuan et al. [25,26]. Here, the validity of this result requires that the infinite matrix surrounding the inclusion is homogeneous. However, the fact is that a bulk material may contain many internal microdefects (like dislocations, micro-cracks or grain boundaries), and it is reasonably anticipated that an elliptical inclusion no longer enjoys the constant-stress feature if a microdefect in the matrix appears near it. A question then arises: how does an elliptical inclusion evolve to maintain its internal constant stress when encountering a microdefect in the surrounding environment? To answer this question, one would inevitably encounter some inverse problems of the parameterization and identification of the domain of definition of certain potential functions. Such inverse problems are usually much more challenging than their forward counterparts, in which the objective is to determine the stress field for given domain of definition of the potential functions, especially when analytic or semi-analytic solutions are required to ensure a high accuracy of recovering the configuration of the corresponding domain of definition.

In the literature, there have been only few pieces of work on the identification of the inclusion shape allowing for a uniform internal stress field in the presence of a nearby microdefect. For example, in the context of anti-plane shear deformations, Wang et al. [27] devised an ingenious mapping function to derive explicit solutions for a certain family of the geometry of a uniformly stressed inclusion interacting with a screw dislocation, and they subsequently extended their essential idea to develop an analytic procedure of determining the shape of an inclusion with constant stress nearby a straight mode-III crack [28], while Dai et al. [29] resorted to the existence theorem of holomorphic functions with specified-form boundary values and proposed a unified analytic algorithm for identifying the shape of an inclusion with uniform stress in the vicinity of a screw dislocation whether the inclusion-matrix interface is treated as being perfectly or imperfectly bonded.

In this paper, we are mainly concerned with the existence of a constant stress field inside an inclusion when it verges on a material interface. From a technical point of view, we need to classify the corresponding inverse problem into two categories. In the first category, the geometry of the material interface is not fixed, and both it and that of the inclusion-matrix interface are adjustable to make the stress inside the inclusion uniform. In the second category, however, the geometry of the material interface is specified in advance and that of the inclusion-matrix is then the only variable in the process of attaining the uniformity of the stress inside the inclusion. In short, the second category contains fewer degrees of freedom than the first one in designing a uniformly stressed inclusion nearby a material interface, and in this case, to the authors' experience in analytically solving similar inverse problems, it would be more intractable than the first one. For example, Wang et al. [30] invented a special mapping function for the first-category design of the shape of an inclusion ensuring the uniformity of the stress within it when it is embedded in a bi-material composite composed of two infinite elastic half-planes with a certain wavy interface, although if one requires that the interface between the two half-planes is flat, the mapping function would be not applicable and particularly it remains unclear how to devise an appropriate mapping function. More typical examples for the first-category problems involving the interaction between a closed material interface and an inclusion with constant stress can be found in Refs. [22,31-35], in which two or more adjacent inclusions were investigated and all of the inclusion-matrix interfaces were treated as variables that were identified to guarantee a constant internal stress field for each inclusion. So far in the literature, however, we have not found any piece of research on the strict second-category problems. Nevertheless, one may find in the literature some results for the limiting case of a second-category problem in which the material interface reduces to a traction-free material boundary. For example, in Refs. [36,37], the authors developed analytic procedures to determine the configuration of multiple inclusions each enveloping a constant stress field in the vicinity of a flat traction-free surface of an elastic half-plane where the inclusions are embedded. It is also worth mentioning some pieces of work concentrating on certain weak versions of the second-category problems in which the material interface of specified shape in a matrix is roughly modelled by applying an eigenstrain to a subdomain of the matrix. For example, in the deformations of anti-plane shear, Wang et al. [38,39]

determined the shape for a single inclusion holding a uniform stress in an infinite matrix when a circular Eshelby inclusion (of the same shear modulus as that of the matrix) with either a constant or linear eigenstrain appears in its neighborhood. From a theoretical point of view, a general circular inclusion (of distinct elastic constants from those of the matrix) may be equivalently replaced by a circular Eshelby inclusion with a certain eigenstrain, although the specific eigenstrain ensuring the equivalence of replacement depends strongly on the details of external loadings and especially on the geometry and distribution of other defects or inclusions (if any). Consequently, for the problems addressed in Refs. [38,39], the introduction of either constant or linear eigenstrain could never guarantee the exact equivalence between a general circular inclusion and a circular Eshelby inclusion, and particularly appropriate eigenstrains allowing for the exact equivalence should be treated as unknowns to be ascertained with the determination of the shape of the uniformly stressed inclusion. Recent literature reported also a particular weak version of the second-category problems in which the material interface of specified shape (the Booth's lemniscate or cardioid) nearby the inclusion (designed to admit a constant internal field) is degenerated to such an extent that the materials on the two sides of the interface have the same shear modulus but distinct Poisson's ratios [40]. In this paper, we endeavor to extend the results in Ref. [36] to the case of an inclusion with constant stress embedded in two bonded elastic half-planes with a straight interface, which forms a strict, non-degenerate second-category problem.

We arrange the following content of the paper into four parts. In the first one, we introduce basic equations for the anti-plane shear deformation of an inclusion with a uniform anti-plane shear eigenstrain placed into an infinite bi-material system made up of two semi-infinite elastic half-planes, and give a mathematical description for the corresponding inverse problem of identifying the geometry of the inclusion when the eigenstrain-induced stress inside it is required to be a constant. In the second one, we present two methods to derive the essential equation that the geometry of the inclusion needs to satisfy to attain the desired constant internal stress, and explain the solution procedure for such an equation. In the third one, numerical results for some admissible shapes of the inclusion are illustrated, and the influence of the stiffness of the bi-material interface on the shape of the inclusion is discussed. Finally, the main points of the problem, the solution and results are mentioned in the last part.

## 2. Details of the inverse problem

By referring to the Cartesian $x_1$-$x_2$ coordinate system, we consider a bi-material structure composed of two elastic half-planes bonded together perfectly via an infinitely long straight interface, in the context of the theory of linear isotropic elasticity. An inclusion with a uniform anti-plane shear eigenstrain is introduced into the lower half-plane, and the entire composite system, as diagramed in Fig. 1, is assumed to be under the anti-plane shear deformation and free of any other external loadings except for the eigenstrain exerted on the inclusion. Here, for the lower half-plane, we assume theoretically that the inclusion has the same shear modulus as that of its surrounding lower matrix (i.e., the entire lower half-plane has a unified shear modulus) since the eigenstrain contained in it may represent to a considerable extent the difference between the shear moduli of the inclusion and matrix in practical situations, while for the upper half-plane its shear modulus is allowed to be distinct from that of the lower half-plane. We denote the upper half-plane region and the complete lower half-plane region by $S_{\mathrm{U}}$ and $S_{\mathrm{L}}$, the inclusion region and the lower matrix region by $S_{\mathrm{in}}$ and $S_{\mathrm{LM}}$, and the bi-material interface between the two half-planes and the inclusion-matrix interface by $L_{\mathrm{b}}$ and $L_{\mathrm{in}}$. We also introduce in the upper half-plane an auxiliary region denoted by $S_{\mathrm{Uin}}$ and an auxiliary closed curve denoted by $L_{\mathrm{Uin}}$, which are symmetric, respectively, to $S_{\mathrm{in}}$ and $L_{\mathrm{in}}$ in the lower half-plane. The shear moduli of the upper and lower half-planes are denoted by $G_{\mathrm{U}}$ and $G_{\mathrm{L}}$. We particularly use the index "3" to represent the $x_3$-diretion perpendicular to the $x_1$-$x_2$ plane, and therefore the Cartesian components of the uniform eigenstrain imposed on the inclusion are described by $\varepsilon_{13}^*$ and $\varepsilon_{23}^*$.

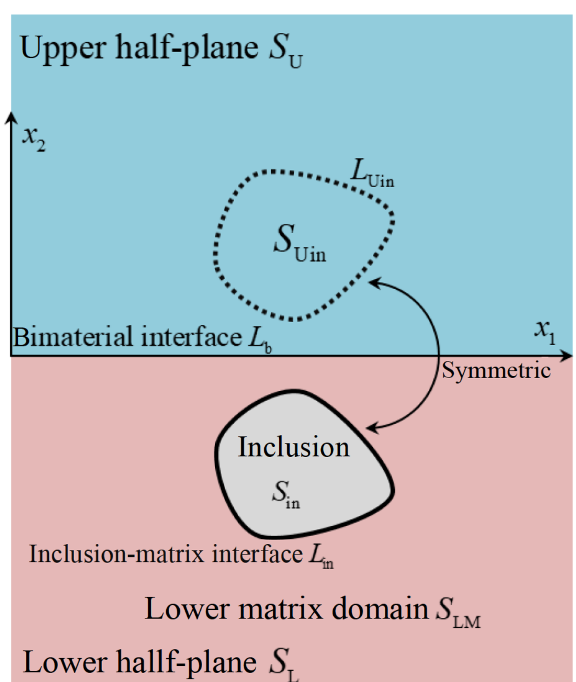


**Figure 1** An inclusion nearby a long straight bi-material interface in anti-plane shear.

Distinct from many forward problems in which the main objective is to determine the stress field induced by the eigenstrain in the entire composite system when the geometry of the inclusion is given in advance, the current problem focuses on the inverse case in which the eigenstrain-induced stress is required to keep a constant within the entire inclusion and the geometry of the inclusion is identified to achieve this requirement.

To formulate the above-mentioned inverse problem mathematically, we recall the well-known complex formalism for anti-plane shear elasticity. In fact, since the intrinsic governing equation for the anti-plane shear deformation in elastostatics is a two-dimensional Laplace equation, the out-of-plane displacement $u_3$ and the anti-plane shear components ($\sigma_{13}$, $\sigma_{23}$) of the stress tensor could be represented in terms of an analytic function $f(z)$ ($z = x_1 + \mathrm{i}x_2$, i is the imaginary unit) defined in the elastic domain under consideration. The specific representation for each component of the composite system is organized as

$$\left.\begin{aligned} u_3^{(k)} &= \mathrm{Im}[f_k(z)], \\ \sigma_{23}^{(k)} + \mathrm{i}\sigma_{13}^{(k)} &= G_k f_k'(z), \end{aligned}\right\} z \in S_k,\ (k = \text{“U”, “LM” or “in”}), \tag{1}$$

where

$$G_{\mathrm{LM}} = G_{\mathrm{in}} = G_{\mathrm{L}}, \tag{2}$$

and the indices “U”, “LM” and “in” are introduced to identify the corresponding quantities in the upper half-plane, the lower matrix and the inclusion, respectively. Here, the $f$-related functions introduced from Eq. (1) are all analytic functions in their respective domains of definition, and particularly we may stipulate in advance that

$$\lim_{|z|\to\infty} f_{\mathrm{LM}}(z) = 0,\ z \in S_{\mathrm{LM}}, \tag{3}$$

in order to make the solution for each of these analytic functions unique when the geometry of the inclusion is determined.

The boundary conditions on the bi-material interface $L_{\mathrm{b}}$ describing the continuity of the traction (i.e., the $\sigma_{23}$-com--component) and displacement across the interface are expressed using $f_{\mathrm{U}}(z)$ and $f_{\mathrm{LM}}(z)$ as [34]

$$f_{\mathrm{LM}}(t) = \frac{1}{2}\left(1 + \frac{G_{\mathrm{U}}}{G_{\mathrm{L}}}\right) f_{\mathrm{U}}(t) + \frac{1}{2}\left(\frac{G_{\mathrm{U}}}{G_{\mathrm{L}}} - 1\right)\overline{f_{\mathrm{U}}(t)},\ t \in L_{\mathrm{b}}, \tag{4}$$

which combined with Eq. (3) indicates

$$\lim_{|z|\to\infty} f_{\mathrm{U}}(z) = 0,\ z \in S_{\mathrm{U}}. \tag{5}$$

On the inclusion-matrix interface $L_{\mathrm{in}}$, similar boundary conditions are established as [36]

$$f_{\mathrm{LM}}(t) = f_{\mathrm{in}}(t) + \Gamma^* t - \overline{\Gamma}^* \overline{t},\ t \in L_{\mathrm{in}}, \tag{6}$$

where

$$\Gamma^* = \varepsilon_{23}^* + \mathrm{i}\varepsilon_{13}^*. \tag{7}$$

Here, Eqs. (4) and (6) differ in the form mainly because the inclusion and lower matrix have the same shear modulus and specially the displacement in the inclusion should be interpreted as the combination of the stress-related displacement and the eigenstrain-caused displacement. Since a constant stress is required within the inclusion, $f_{\mathrm{in}}(z)$ has to be

$$f_{\mathrm{in}}(z) = \Gamma_{\mathrm{in}} z + C,\ \forall z \in S_{\mathrm{in}}, \tag{8}$$

where $\Gamma_{\mathrm{in}}$ is a complex number characterizing the uniform stress-caused strain inside the inclusion, and $C$ is a certain constant ensuring the fulfillment of all the boundary conditions. Substituting Eq. (8) into Eq. (6), we organize the boundary value of $f_{\mathrm{LM}}(z)$ on $L_{\mathrm{in}}$ into

$$f_{\mathrm{LM}}(t) = At + B\overline{t} + C,\ t \in L_{\mathrm{in}}, \tag{9}$$

with

$$A = \Gamma_{\mathrm{in}} + \Gamma^*,\ B = -\overline{\Gamma}^*. \tag{10}$$

Now in the context of the complex formalism and the boundary conditions presented above, we describe the current inverse problem as to find an appropriate geometry of $L_{\mathrm{in}}$ such that the analytic functions $f_{\mathrm{LM}}(z)$ and $f_{\mathrm{U}}(z)$ could exist (in their respective domains of definition) under the constraints given in Eqs. (3)-(5) and (9). In what follows, we show how to establish the equations with respect to the geometry of the inclusion, respectively, from analytic continuation techniques and existence theorems of analytic functions with specified-form boundary values, and from the Green’s function of a concentrated force imposed on the bi-material structure of two bonded half-planes.

## 3. Geometrical equations of the inclusion

### 3.1 Analytic continuation and existence theorem of analytic functions

We introduce an auxiliary function $Q(z)$ defined in the union of $S_{\mathrm{LM}}$ and $S_{\mathrm{U}}$ as

$$Q(z) = \begin{cases} f_{\mathrm{LM}}(z) - \dfrac{1}{2}\left(\dfrac{G_{\mathrm{U}}}{G_{\mathrm{L}}} - 1\right)\overline{f_{\mathrm{U}}(\overline{z})}, & z \in S_{\mathrm{LM}}, \\ \dfrac{1}{2}\left(1 + \dfrac{G_{\mathrm{U}}}{G_{\mathrm{L}}}\right) f_{\mathrm{U}}(z), & z \in S_{\mathrm{U}}. \end{cases} \tag{11}$$

Noting Eq. (4), one readily sees that $Q(z)$ is analytic everywhere in $S_{\mathrm{LM}} \cup S_{\mathrm{U}}$ (including the neighborhood of the bi-material interface $L_{\mathrm{b}}$) despite that it is expressed in terms of a piecewise function. In particular, it follows from Eqs. (3) and (5) that

$$\lim_{|z|\to\infty} Q(z) = 0,\ z \in S_{\mathrm{LM}} \cup S_{\mathrm{U}}. \tag{12}$$

The existence of $f_{\mathrm{LM}}(z)$ and $f_{\mathrm{U}}(z)$ subjected to Eqs. (3)-

(5) and (9) is then transformed equivalently into that of $Q(z)$ and $f_{\mathrm{U}}(z)$ subjected to Eqs. (5), (12) and

$$Q(t) = At + B\bar{t} + C - \frac{1}{2}\left(\frac{G_{\mathrm{U}}}{G_{\mathrm{L}}} - 1\right)\overline{f_{\mathrm{U}}(\bar{t})},\ t \in L_{\mathrm{in}}. \tag{13}$$

Applying the existence theorem of an analytic function to $Q(z)$ complying with Eqs. (12) and (13), we obtain

$$\frac{1}{2\pi \mathrm{i}}\oint_{L_{\mathrm{in}}} \frac{At + B\bar{t} + C - \frac{1}{2}\left(\frac{G_{\mathrm{U}}}{G_{\mathrm{L}}} - 1\right)\overline{f_{\mathrm{U}}(\bar{t})}}{t - z}\mathrm{d}t = 0,\ \forall z \in S_{\mathrm{in}}. \tag{14}$$

Using the Cauchy's integral formula and noticing the analyticity of $\overline{f_{\mathrm{U}}(\bar{z})}$ in $S_{\mathrm{in}}$, one could simplify Eq. (14) into

$$\frac{1}{2}\left(\frac{G_{\mathrm{U}}}{G_{\mathrm{L}}} - 1\right)\overline{f_{\mathrm{U}}(\bar{z})} = Az + \frac{B}{2\pi \mathrm{i}}\oint_{L_{\mathrm{in}}}\frac{\bar{t}}{t-z}\mathrm{d}t + C, \tag{15}$$

$\forall z \in S_{\mathrm{in}}$,

which can be rewritten equivalently as

$$\frac{1}{2}\left(\frac{G_{\mathrm{U}}}{G_{\mathrm{L}}} - 1\right)f_{\mathrm{U}}(z) = \bar{A}z - \frac{\bar{B}}{2\pi \mathrm{i}}\oint_{L_{\mathrm{in}}}\frac{t}{\bar{t}-z}\mathrm{d}\bar{t} + \bar{C},\ \forall z \in S_{\mathrm{Uin}}, \tag{16}$$

where the specific form of $f_{\mathrm{U}}(z)$ within $S_{\mathrm{Uin}}$ shown in Eq. (16) is obtained directly from the existence principle of $Q(z)$ subjected to Eqs. (12) and (13). In contrast, we provide another perspective to evaluate $f_{\mathrm{U}}(z)$ in the entire $S_{\mathrm{U}}$. In fact, since $Q(z)$ vanishes at any infinity point and its domain of definition (i.e., $S_{\mathrm{LM}} \cup S_{\mathrm{U}}$) has only one internal boundary (i.e., $L_{\mathrm{in}}$), one may easily recover the value of $Q(z)$ at any point within the domain from its boundary value given in Eq. (13). Additionally noticing the fact that $\overline{f_{\mathrm{U}}(\bar{z})}$ is analytic in $S_{\mathrm{in}}$ while $S_{\mathrm{in}}$ has no intersection with the union of $S_{\mathrm{LM}}$ and $S_{\mathrm{U}}$, we determine $Q(z)$ immediately as

$$Q(z) = -\frac{B}{2\pi \mathrm{i}}\oint_{L_{\mathrm{in}}}\frac{\bar{t}}{t-z}\mathrm{d}t,\ \forall z \in S_{\mathrm{LM}} \cup S_{\mathrm{U}}. \tag{17}$$

Equating Eq. (17) and the specific expression of $Q(z)$ in $S_{\mathrm{U}}$ introduced from Eq. (11) leads to

$$\frac{1}{2}\left(1 + \frac{G_{\mathrm{U}}}{G_{\mathrm{L}}}\right)f_{\mathrm{U}}(z) = -\frac{B}{2\pi \mathrm{i}}\oint_{L_{\mathrm{in}}}\frac{\bar{t}}{t-z}\mathrm{d}t,\ \forall z \in S_{\mathrm{U}}, \tag{18}$$

which gives the unified form of $f_{\mathrm{U}}(z)$ in the entire $S_{\mathrm{U}}$.

It is easily found that the existence of $f_{\mathrm{U}}(z)$ requires necessarily and depends sufficiently on that the two versions of $f_{\mathrm{U}}(z)$ arising from Eqs. (16) and (18) are consistent in the entire $S_{\mathrm{Uin}}$. Consequently, one has

$$\bar{A}z - \frac{\bar{B}}{2\pi \mathrm{i}}\oint_{L_{\mathrm{in}}}\frac{t}{\bar{t}-z}\mathrm{d}\bar{t} + \frac{\alpha B}{2\pi \mathrm{i}}\oint_{L_{\mathrm{in}}}\frac{\bar{t}}{t-z}\mathrm{d}t + \bar{C} = 0,\ \forall z \in S_{\mathrm{Uin}}, \tag{19}$$

where

$$\alpha = \frac{G_{\mathrm{U}} - G_{\mathrm{L}}}{G_{\mathrm{U}} + G_{\mathrm{L}}}. \tag{20}$$

Since $S_{\mathrm{Uin}}$ and $S_{\mathrm{in}}$ are symmetric about the real axis ($x$-axis), we obtain by conjugating Eq. (19) that

$$Az + \frac{B}{2\pi \mathrm{i}}\oint_{L_{\mathrm{in}}}\frac{\bar{t}}{t-z}\mathrm{d}t - \frac{\alpha \bar{B}}{2\pi \mathrm{i}}\oint_{L_{\mathrm{in}}}\frac{t}{\bar{t}-z}\mathrm{d}\bar{t} + C = 0,\ \forall z \in S_{\mathrm{in}}. \tag{21}$$

Now we arrive at the integral Eq. (21) with respect to the geometry of $L_{\mathrm{in}}$ which can be used to determine the configuration of the inclusion when it achieves a uniform stress field.

It is worth noting that Eq. (21) is not only a necessary condition but also a sufficient condition for the existence of a uniformly stressed inclusion interacting with the straight bi-material interface. In fact, following the routine of analysis presented above, one could easily construct $f_{\mathrm{LM}}(z)$ and $f_{\mathrm{U}}(z)$ as

$$f_{\mathrm{LM}}(z) = \frac{\alpha \bar{B}}{2\pi \mathrm{i}}\oint_{L_{\mathrm{in}}}\frac{t}{\bar{t}-z}\mathrm{d}\bar{t} - \frac{B}{2\pi \mathrm{i}}\oint_{L_{\mathrm{in}}}\frac{\bar{t}}{t-z}\mathrm{d}t,\ z \in S_{\mathrm{LM}}, \tag{22}$$

$$f_{\mathrm{U}}(z) = -\frac{G_{\mathrm{L}}B}{\pi \mathrm{i}(G_{\mathrm{L}} + G_{\mathrm{U}})}\oint_{L_{\mathrm{in}}}\frac{\bar{t}}{t-z}\mathrm{d}t,\ z \in S_{\mathrm{U}}, \tag{23}$$

which are analytic in their respective domains of definition, vanish at all the corresponding infinity points, and meet the boundary condition Eq. (4) automatically. When Eq. (21) holds, one has

$$\frac{\alpha \bar{B}}{2\pi \mathrm{i}}\oint_{L_{\mathrm{in}}}\frac{t}{\bar{t}-t_1}\mathrm{d}\bar{t} = At_1 + g^{+}(t_1) + C,\ t_1 \in L_{\mathrm{in}}, \tag{24}$$

where

$$g(z) = \frac{B}{2\pi \mathrm{i}}\oint_{L_{\mathrm{in}}}\frac{\bar{t}}{t-z}\mathrm{d}t, \tag{25}$$

and $g^{+}(t_1)$ represents the limit of $g(z)$ when $z$ tends towards $t_1$ from the inside of $L_{\mathrm{in}}$. The boundary value of $f_{\mathrm{LM}}(z)$ on $L_{\mathrm{in}}$ is read from Eq. (22) as

$$f_{\mathrm{LM}}(t_1) = \frac{\alpha \bar{B}}{2\pi \mathrm{i}}\oint_{L_{\mathrm{in}}}\frac{t}{\bar{t}-t_1}\mathrm{d}\bar{t} - g^{-}(t_1),\ t_1 \in L_{\mathrm{in}}, \tag{26}$$

where $g^{-}(t_1)$ denotes the limit of $g(z)$ when $z$ moves towards $t_1$ from the outside of $L_{\mathrm{in}}$. Substituting Eq. (24) into Eq. (26) and using the Plemelj formula,

$$g^{+}(t_1) - g^{-}(t_1) = B\bar{t}_1,\ t_1 \in L_{\mathrm{in}}, \tag{27}$$

we find

$$f_{\mathrm{LM}}(t_1) = At_1 + B\bar{t}_1 + C,\ t_1 \in L_{\mathrm{in}}, \tag{28}$$

which agrees with Eq. (9). Now we confirm that Eq. (21) does serve as a sufficient condition ensuring the existence of a constant stress inside the inclusion nearby the bi-material interface $L_{\mathrm{b}}$.

### 3.2 Green's function method

The use of the Green's functions is a more direct way of deriving the essential equations of the geometry of the inclusion that occupies a uniform stress field nearby the straight bi-material interface. Let us consider, as depicted in Fig. 2, the case of a bi-material structure made up of two homogeneous elastic half-planes (without any inclusion), in which the two half-planes are perfectly bonded through a straight interface and the lower half-plane undergoes an out-of-plane concentrated force $P$ at the point $z_c$. The Green's function for this case is usually referred to as the solution for the stress field induced by the concentrated force in the entire structure.

The Green's function for the concentrated force considered here is similar to that for a screw dislocation located in the same bi-material structure, which may be found in Ref. [41]. Consequently, the former could be achieved easily by modifying the latter slightly, and we present it (denoted by $G(z,P,z_c)$) as

$$G(z,P,z_c)=\begin{cases} f_{\rm U}'(z)=\dfrac{P}{\pi{\rm i}(G_{\rm U}+G_{\rm L})(z-z_c)}, & z\in S_{\rm U},\\[2ex] f_{\rm L}'(z)=\dfrac{P}{2\pi{\rm i}G_{\rm L}}\left(\dfrac{1}{z-z_c}-\dfrac{\alpha}{z-\bar z_c}\right), & z\in S_{\rm L},\end{cases} \tag{29}$$

where a similar notation (see Sect. 2) is used to represent related analytic functions and shear moduli and $\alpha$ is again defined from Eq. (20). Here, Eq. (29) may be also obtained via directly applying the Cauchy's integral formula to the perfect bonding condition (similar to that given in Eq. (4)) on the bi-material interface $L_{\rm b}$. In addition, the validity of Eq. (29) lies in that it indeed leads to the continuity of the $\sigma_{23}$-component of the stress and the $x$-gradient of the displacement across the bi-material interface.

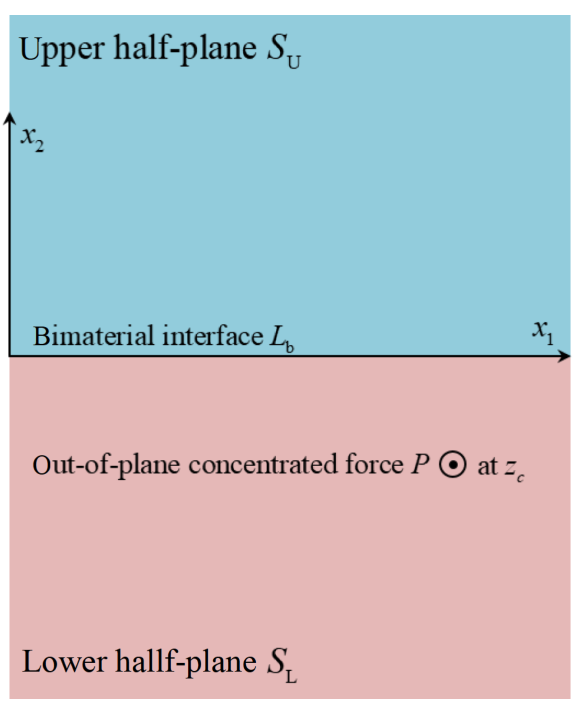


**Figure 2** An out-of-plane (anti-plane) concentrated force acting on the lower half-plane of the bi-material system free of any inclusion.

Let us go back to the original problem of the three-component composite system established in Sect. 2. Since the inclusion and the lower matrix share a common shear modulus, the uniform eigenstrain-induced stress field can be acquired conveniently for each component of the composite system via the utilization of the Green's function represented by Eq. (29). In fact, based on the principle of superposition for treating eigenstrained inclusion problems (introduced from Eshelby's seminal paper), when an appropriate distributed loading $p$ is additionally exerted on the inclusion-matrix interface $L_{\rm in}$ to prevent the eigenstrained inclusion from interacting with the remaining components of the composite system, the lower matrix and upper half-plane would both become stress-free while the inclusion would occupy a constant strain that is just opposite to the eigenstrain. According to the uniqueness of the solution for a boundary-value problem in linear elasticity, it is easy to find the satisfactory distributed loading $p(t)$ ($t\in L_{\rm in}$) as

$$p(t)=G_{\rm L}{\rm Re}\left(2\Gamma^*\frac{{\rm d}t}{{\rm d}s}\right)=G_{\rm L}\left(\Gamma^*\frac{{\rm d}t}{{\rm d}s}+\bar\Gamma^*\frac{{\rm d}\bar t}{{\rm d}s}\right),\ t\in L_{\rm in}, \tag{30}$$

where ${\rm d}t$ is an infinitesimal complex quantity characterizing an infinitesimal counterclockwise-directed element of the curve $L_{\rm in}$, and ${\rm d}s$ denotes the length of it. The consequences of performing the above-mentioned principle of superposition are organized into

$$f_k'(z)+\oint_{L_{\rm in}}G(z,p(t)\cdot{\rm d}s,t)=0,\ z\in S_k,\ (k=\text{“U” or “LM”}), \tag{31}$$

$$f_{\rm in}'(z)+\oint_{L_{\rm in}}G(z,p(t)\cdot{\rm d}s,t)=-2\Gamma^*,\ z\in S_{\rm in}. \tag{32}$$

Substituting Eq. (29) into Eqs. (31) and (32), and employing the Cauchy's integral formula, we acquire the general solutions to the three analytic functions for an arbitrary shape of the inclusion as

$$f_{\rm LM}'(z)=\frac{\bar\Gamma^*}{2\pi{\rm i}}\oint_{L_{\rm in}}\frac{{\rm d}\bar t}{t-z}-\frac{\alpha\Gamma^*}{2\pi{\rm i}}\oint_{L_{\rm in}}\frac{{\rm d}t}{\bar t-z},\ z\in S_{\rm LM}, \tag{33}$$

$$f_{\rm U}'(z)=\frac{G_{\rm L}\bar\Gamma^*}{\pi{\rm i}(G_{\rm U}+G_{\rm L})}\oint_{L_{\rm in}}\frac{{\rm d}\bar t}{t-z},\ z\in S_{\rm U}, \tag{34}$$

$$f_{\rm in}'(z)=-\Gamma^*+\frac{\bar\Gamma^*}{2\pi{\rm i}}\oint_{L_{\rm in}}\frac{{\rm d}\bar t}{t-z}-\frac{\alpha\Gamma^*}{2\pi{\rm i}}\oint_{L_{\rm in}}\frac{{\rm d}t}{\bar t-z},\ z\in S_{\rm in}. \tag{35}$$

Since $L_{\rm in}$ is a closed curve, we apply the integration by parts to each of the contour integrals in Eqs. (33)-(35) and then arrive at

$$f_{\rm LM}'(z)=\frac{\overline{\Gamma^*}}{2\pi{\rm i}}\oint_{L_{\rm in}}\frac{\bar{t}}{(t-z)^2}{\rm d}t-\frac{\alpha\Gamma^*}{2\pi{\rm i}}\oint_{L_{\rm in}}\frac{t}{(\bar{t}-z)^2}{\rm d}\bar{t},\ z\in S_{\rm LM},\tag{36}$$

$$f_{\rm U}'(z)=\frac{G_{\rm L}\overline{\Gamma^*}}{\pi{\rm i}(G_{\rm U}+G_{\rm L})}\oint_{L_{\rm in}}\frac{\bar{t}}{(t-z)^2}{\rm d}t,\ z\in S_{\rm U},\tag{37}$$

$$\begin{aligned}f_{\rm in}'(z)=&-\Gamma^*+\frac{\overline{\Gamma^*}}{2\pi{\rm i}}\oint_{L_{\rm in}}\frac{\bar{t}}{(t-z)^2}{\rm d}t\\&-\frac{\alpha\Gamma^*}{2\pi{\rm i}}\oint_{L_{\rm in}}\frac{t}{(\bar{t}-z)^2}{\rm d}\bar{t},\ z\in S_{\rm in},\end{aligned}\tag{38}$$

whose integrals with respect to $z$ turn out to be, respectively, as

$$f_{\rm LM}(z)=\frac{\overline{\Gamma^*}}{2\pi{\rm i}}\oint_{L_{\rm in}}\frac{\bar{t}}{t-z}{\rm d}t-\frac{\alpha\Gamma^*}{2\pi{\rm i}}\oint_{L_{\rm in}}\frac{t}{\bar{t}-z}{\rm d}\bar{t},\ z\in S_{\rm LM},\tag{39}$$

$$f_{\rm U}(z)=\frac{G_{\rm L}\overline{\Gamma^*}}{\pi{\rm i}(G_{\rm U}+G_{\rm L})}\oint_{L_{\rm in}}\frac{\bar{t}}{t-z}{\rm d}t,\ z\in S_{\rm U},\tag{40}$$

$$\begin{aligned}f_{\rm in}(z)=&-\Gamma^*+\frac{\overline{\Gamma^*}}{2\pi{\rm i}}\oint_{L_{\rm in}}\frac{\bar{t}}{t-z}{\rm d}t\\&-\frac{\alpha\Gamma^*}{2\pi{\rm i}}\oint_{L_{\rm in}}\frac{t}{\bar{t}-z}{\rm d}\bar{t}-C,\ z\in S_{\rm in}.\end{aligned}\tag{41}$$

Here, we simply follow the stipulation given in Eq. (3) and neglect the integration constant in recovering $f_{\rm LM}(z)$ from Eq. (36), and in this case we have to obey Eq. (5) when recovering $f_{\rm U}(z)$ from Eq. (37), although we do need to retain an integration constant $C$ for $f_{\rm in}(z)$ in Eq. (41), otherwise the displacement may undergo a constant jump across the inclusion-matrix interface $L_{\rm in}$ (because the Green's function given in Eq. (29) is directly related to the stress or the gradients of the displacement not the displacement itself). In particular, one may find that Eqs. (39) and (40) derived by the Green's function method are consistent with those obtained in Eqs. (22) and (23) by the analytic continuation techniques and existence theorem of analytic functions.

If the stress field inside the inclusion is required to be uniform, we only need to specify $f_{\rm in}(z)$ as a linear function (for example, let $f_{\rm in}(z)=\Gamma_{\rm in}z$), in which the constant term is negligible since we have already included a certain $C$ in Eq. (41). In this case, Eq. (41) becomes

$$(\Gamma_{\rm in}+\Gamma^*)z-\frac{\overline{\Gamma^*}}{2\pi{\rm i}}\oint_{L_{\rm in}}\frac{\bar{t}}{t-z}{\rm d}t+\frac{\alpha\Gamma^*}{2\pi{\rm i}}\oint_{L_{\rm in}}\frac{t}{\bar{t}-z}{\rm d}\bar{t}+C=0,\ z\in S_{\rm in},\tag{42}$$

which imposes a constraint condition on the geometry of the inclusion and appears to be exactly the same as the one established in Sect. 3.1 (see Eq. (21) there). Specially, in the context of the Green's function method, Eq. (42) is obviously a sufficient and necessary condition related to the existence of a constant stress inside the inclusion because Eqs. (39)-(41) are general solutions for an arbitrarily-shaped inclusion with uniform eigenstrain embedded in the system of two bonded elastic half-planes.

### 3.3 Solution procedure

In general, it is of formidable difficulty to extract a closed-form expression for the configuration of the curve $L_{\rm in}$ from the integral-type Eq. (21) or (42). We take a procedure of combining analytic and numerical techniques to find a series-form solution for the configuration of $L_{\rm in}$ satisfying Eq. (21) or (42).

Firstly, we prescribe the overall position and size of the inclusion in advance by specifying a complex quantity $z_{\rm in}$ and a real positive number $R_{\rm in}$, and parameterize the shape of the inclusion by a group of unknown complex constants $a_j$ $(j=1,2,3,...)$. Using conformal mapping techniques, we represent the geometry of $L_{\rm in}$ as [42]

$$t\in L_{\rm in}:\ t=\omega(\sigma)=z_{\rm in}+R_{\rm in}\left(\sigma+\sum_{j=1}^{\infty}a_j\sigma^{-j}\right),\quad \sigma={\rm e}^{{\rm i}\theta},\ (0\le\theta<2\pi).\tag{43}$$

Then, one could expand the contour integrals on the left side of Eq. (21) in terms of the Faber polynomials $F_j(z)$ $(j=1,2,3,...)$ of the simply-connected domain $S_{\rm in}$. The zero-order and first-order Faber polynomials are

$$F_0(z)=1,\ F_1(z)=\frac{z-z_{\rm in}}{R_{\rm in}},\ z\in S_{\rm in},\tag{44}$$

whose form does not rely on the details of the shape of $S_{\rm in}$, while their high-order counterparts depend on the shape parameters $a_j$ $(j=1,2,3,...)$ and can be established via a recurrence relation as [43]

$$F_{j+1}(z)=F_1(z)F_j(z)-\sum_{k=1}^{j-1}a_kF_{j-k}(z)-(j+1)a_j,\ j=1,2,3,...\tag{45}$$

For the first contour integral of Eq. (21), one may easily derive its explicit Faber series expansion as

$$\frac{1}{2\pi{\rm i}}\oint_{L_{\rm in}}\frac{\bar{t}}{t-z}{\rm d}t=\bar{z}_{\rm in}F_0(z)+R_{\rm in}\sum_{j=1}^{\infty}\bar{a}_jF_j(z),\ z\in S_{\rm in},\tag{46}$$

although for the second one, one usually cannot avoid introducing a group of double integrals in finding the coefficients of the corresponding Faber series. According to the definition of the coefficients of a Faber series, we organize the Faber series expansion of the second contour integral in Eq. (21) as

$$\frac{1}{2\pi i}\oint_{L_{in}}\frac{t}{\bar{t}-z}d\bar{t} = R_{in}\sum_{j=0}^{\infty} b_j F_j(z), \tag{47}$$

where

$$b_j = \frac{1}{4\pi^2}\oint_{|\eta|=1}\left(\oint_{|\sigma|=1}\frac{\omega_n(\sigma)\overline{\omega_n'(\sigma)}\sigma^{-2}}{\overline{\omega_n(\sigma)}-\omega_n(\eta)}d\sigma\right)\eta^{-j-1}d\eta, \tag{48}$$

with $\omega_n(\chi)$ defined as

$$\omega_n(\chi) = \frac{z_{in}}{R_{in}} + \chi + \sum_{j=1}^{\infty} a_j\chi^{-j}. \tag{49}$$

Now based on the above-introduced Faber series expansion, one may transform Eq. (21) equivalently into a system of nonlinear algebraic equations with respect to the shape parameters $a_j$ $(j = 1,2,3,...)$ and the constant $C$ as

$$\begin{cases} Az_{in}/R_{in} + B\bar{z}_{in}/R_{in} - \alpha\bar{B}b_0 + C/R_{in} = 0, \\ A + B\bar{a}_1 - \alpha\bar{B}b_1 = 0, \\ B\bar{a}_j - \alpha\bar{B}b_j = 0,\ j = 2,3,... \end{cases} \tag{50}$$

Here, the only unknowns involved in Eq. (50) are $a_j$ $(j = 1,2,3,...)$ and $C$ when the eigenstrain-related parameter $\Gamma^*$, the internal constant strain-related parameter $\Gamma_{in}$ and the dimensionless ratio $z_{in}/R_{in}$ are specified in advance. In particular, we prescribe $\Gamma_{in}$ following [36]

$$\Gamma_{in} = -\Gamma^* - g\overline{\Gamma}^*, \tag{51}$$

where $g$ is a complex number that shall be given in advance of a specific calculation. Here, the absolute value and argument of $g$ define, respectively, the aspect ratio and orientation of a uniformly stressed (elliptical) inclusion surrounded by a homogeneous elastic plane containing no material interface, and the logic behind the use of Eq. (51) in defining the uniform stress in the current study is to see how the shape of the classical elliptical inclusion evolves to maintain its specific uniform internal stress when encountering a bi-material interface. In this case, we divide Eq. (50) (excluding the first equation related to $C$ which plays no part in determining the geometry of the inclusion) by $B$ and simply it into

$$\begin{cases} g + \bar{a}_1 - \alpha e^{2i\beta}b_1 = 0, \\ \bar{a}_j - \alpha e^{2i\beta}b_j = 0,\ j = 2,3,... \end{cases} \tag{52}$$

where

$$\beta = \mathrm{Arg}(\Gamma^*). \tag{53}$$

To find a numerical solution for the shape of the inclusion, we truncate Eqs. (43) and (52) by taking $j = 1,2,...,N$ to yield a finite number of unknowns and the same finite number of equations. The truncated version of the nonlinear system (52) could be solved by the Newton-Raphson iterative algorithm with the initial values of $a_j$ $(j = 1,2,...,N)$ set to $a_1 = -\bar{g}$ and $a_j = 0$ for $j \geq 2$. As the central part of the iterative algorithm, the Jacobi matrix can be established readily by applying the chain rule to the specific expression of $b_j$ in Eq. (48). The remaining details of the iterative process are conventional and are disregarded here (one may refer to Ref. [36] for similar details). Generally, as mentioned in Ref. [36], $N = 10$ or so is sufficient for obtaining a reasonably convergent solution for the desired inclusion shape.

We mention two degenerate cases for Eq. (52). In the first one, the upper and lower half-planes have identical shear modulus (i.e., $\alpha = 0$) and thus the solution for Eq. (52) appears to be

$$a_1 = -\bar{g},\ a_j = 0\ (j = 2,3,...),\ \text{for}\ \alpha = 0, \tag{54}$$

which implies an elliptical shape for the uniformly stressed inclusion (this is consistent with the classical result for an inclusion with uniform stress in a homogeneous infinite elastic plane). In the second case, the inclusion is distant from the interface between the two half-planes (i.e., $-\mathrm{Im}(z_{in}) \gg R_{in}$) and thus Eq. (48) approximates to

$$b_j \approx \frac{R_{in}}{8\pi^2\mathrm{Im}(z_{in})}\left(\oint_{L_{in}} t\cdot d\bar{t}\right)\left(\oint_{|\eta|=1}\eta^{-j-1}d\eta\right) = \begin{cases} \dfrac{R_{in}A_{in}}{2\pi\mathrm{Im}(z_{in})}, & j = 0, \\ 0, & j \geq 1, \end{cases} \tag{55}$$

where $A_{in}$ is the area of the inclusion. Consequently, in the second case, Eq. (52) admits the same solution as that described in Eq. (54), indicating that the uniformly stressed inclusion would gradually become elliptical in shape as it moves away from the interface.

## 4. Theoretical and numerical results

It follows from Eqs. (52), (48) and (49) that the shape parameters $a_j$ $(j = 1,2,3,...)$ of the inclusion only depend on the choice of the dimensionless parameters $z_{in}/R_{in}$, $g$, $\alpha e^{2i\beta}$. This indicates that if we take the same combination of the dimensionless parameters in two different cases, then we would obtain identical shapes of the inclusion. Let us consider two cases (identified by I and II), in which the dimensionless parameters satisfy

$$\alpha_I e^{2i\beta_I} = \alpha_{II}e^{2i\beta_{II}},\ \alpha_I \neq \alpha_{II}. \tag{56}$$

It is not difficult to find the fact that Eq. (56) holds only when

$$\alpha_I = -\alpha_{II},\ e^{2i\beta_I} = -e^{2i\beta_{II}}. \tag{57}$$

Noting the specific definition of the parameters in Eq. (57), we read from Eq. (57) that

$$\left(\frac{G_{\rm U}}{G_{\rm L}}\right)_{\rm I}\left(\frac{G_{\rm U}}{G_{\rm L}}\right)_{\rm II}=1,\ (\varepsilon_{23}^*)_{\rm I}(\varepsilon_{23}^*)_{\rm II}+(\varepsilon_{13}^*)_{\rm I}(\varepsilon_{13}^*)_{\rm II}=0. \tag{58}$$

An interesting fact is suggested from Eq. (58) that if a certain inclusion shape allows for a uniform stress inside the inclusion for a material-loading combination described by $(G_{\rm U}/G_{\rm L})_{\rm I}$, $(\varepsilon_{23}^*)_{\rm I}$ and $(\varepsilon_{13}^*)_{\rm I}$, then it could still ensure the uniformity of the stress inside the inclusion when the material-loading combination changes to a different one identified by $(G_{\rm U}/G_{\rm L})_{\rm II}$, $(\varepsilon_{23}^*)_{\rm II}$ and $(\varepsilon_{13}^*)_{\rm II}$ provided the two different material-loading combinations fulfill Eq. (58).

It is implied in the above-mentioned fact that as the bi-material interface becomes stiffer, the evolution of the inclusion's shape that maintains a constant internal stress field depends strongly on the specific plane in which the eigenstrain is applied (hereinafter defined as the plane of the eigenstrain). Figures 3 and 4 illustrate how the shape of the inclusion occupying a uniform stress field changes when the stiffness of the upper half-plane increases. Here, $\alpha=-1$ corresponds to the case, in which the upper half-plane becomes extremely soft and the bi-material interface is thus reduced to a traction-free boundary, while $\alpha=1$ denotes the case in which the shear modulus of the upper half-plane tends towards infinity and therefore the bi-material interface can be treated as a rigid boundary. It is demonstrated from Fig. 3 that as the bi-material interface becomes stiffer (relative to the inclusion) its attraction to the boundary of the nearby inclusion enclosing a constant internal stress increases if the plane of the eigenstrain applied is parallel to it. As observed in Fig. 4, however, the result turns out to be completely opposite (i.e., the attraction between the inclusion and the bi-material interface decreases with increasing relative stiffness of the interface) when the plane of the eigenstrain applied is perpendicular to the bi-material interface.

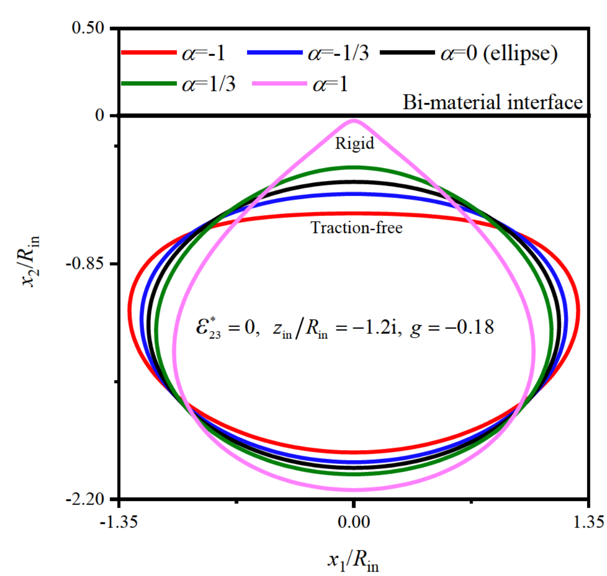


**Figure 3** Configuration of an $\varepsilon_{13}^*$-eigenstrained inclusion achieving constant stress relative to the stiffness of the nearby bi-material interface.

Since the influence of $\varepsilon_{13}^*$ and $\varepsilon_{23}^*$ on the evolution of the inclusion's configuration allowing for a constant internal stress field with increasing stiffness of the bi-material interface are opposite, it is then of particular interest to see what would happen to the configuration of the inclusion as the bi-material interface becomes stiffer when a combined eigenstrain with its two components $\varepsilon_{13}^*$ and $\varepsilon_{23}^*$ having the same magnitude is imposed on the inclusion. An example is shown in Fig. 5. We find that when the two components of

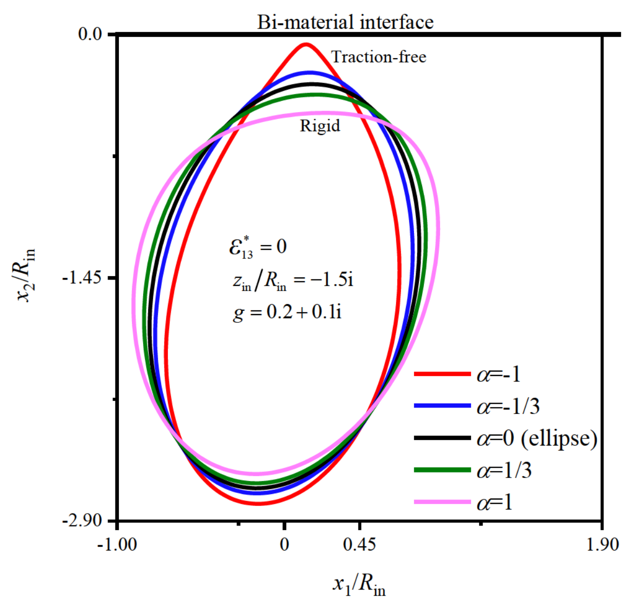


**Figure 4** Configuration of an $\varepsilon_{23}^*$-eigenstrained inclusion with constant stress relative to the stiffness of the nearby bi-material interface.

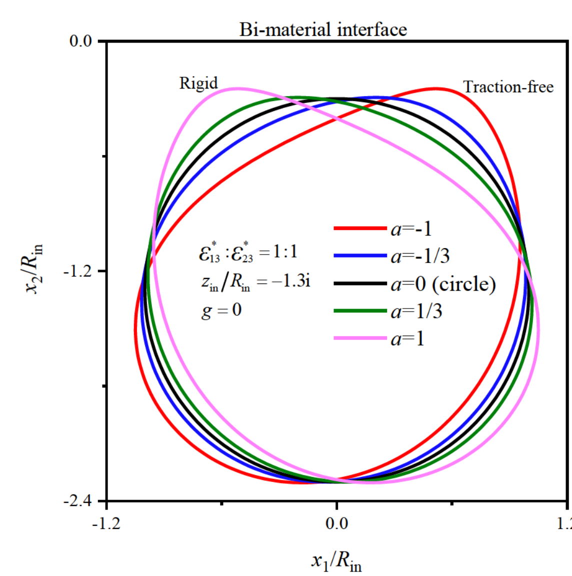


**Figure 5** Configuration of an inclusion occupying constant stress relative to the stiffness of the nearby bi-material interface for a combined eigenstrain.

the eigenstrain applied have an identical magnitude, the varying stiffness of the bi-material interface does not have a great impact on the distance between the interface and the boundary of the inclusion, but instead it influences the orientation of the inclusion significantly.

To validate our theoretical analysis of the uniformly stressed inclusion near the bi-material interface, we conduct finite element simulations for the bi-material structure containing an inclusion whose shape is specified from the current algorithm, and check if the inclusion shape obtained from the theoretical analysis could actually ensure the uniformity of the internal stress inside the inclusion. As a representative example, we take

$$\begin{aligned} &\varepsilon_{23}^* = 0,\ \varepsilon_{13}^* \neq 0,\ z_{\text{in}}/R_{\text{in}} = -1.2\text{i}, \\ &G_{\text{U}}/G_{\text{L}} = 3,\ g = -0.18. \end{aligned} \tag{59}$$

In this case, the configuration of the inclusion (for $N = 10$) is determined as

$$\begin{aligned} t \in L_{\text{in}}:\ t/R_{\text{in}} \approx\ & -1.2\,\text{i} + \sigma + 0.100541196450227 \cdot \sigma^{-1} \\ & -0.0316550509186209 \cdot \text{i}\cdot\sigma^{-2} \\ & +0.0125714473334296 \cdot \sigma^{-3} \\ & +0.00500151893775303 \cdot \text{i}\cdot\sigma^{-4} \\ & -0.00200500707974800 \cdot \sigma^{-5} \\ & -0.000815193839366151 \cdot \text{i}\cdot\sigma^{-6} \\ & +0.000338408989689937 \cdot \sigma^{-7} \\ & +0.000144288490020816 \cdot \text{i}\cdot\sigma^{-8} \\ & -0.0000634451521705119 \cdot \sigma^{-9} \\ & -0.0000288108999554083 \cdot \text{i}\cdot\sigma^{-10}, \end{aligned} \tag{60}$$

and the corresponding desired uniform stress in the inclusion is

$$\sigma_{13}^{(\text{in})} = -1.18 G_{\text{L}}\varepsilon_{13}^*,\ \sigma_{23}^{(\text{in})} = 0,\ \text{in the entire inclusion.} \tag{61}$$

In the finite element simulations, we simply take $G_{\text{U}} = 3$, $G_{\text{L}} = 1$, $\varepsilon_{13}^* = 1$, and $R_{\text{in}} = 1$, and particularly the eigenstrain inside the inclusion is achieved with the setting of anisotropic thermal expansion. The specific geometric model of the bi-material structure containing the inclusion defined geometrically by Eq. (60) is shown in Fig. 6. The simulation results for the two anti-plane shear stress components and the out-of-plane displacement component of the entire

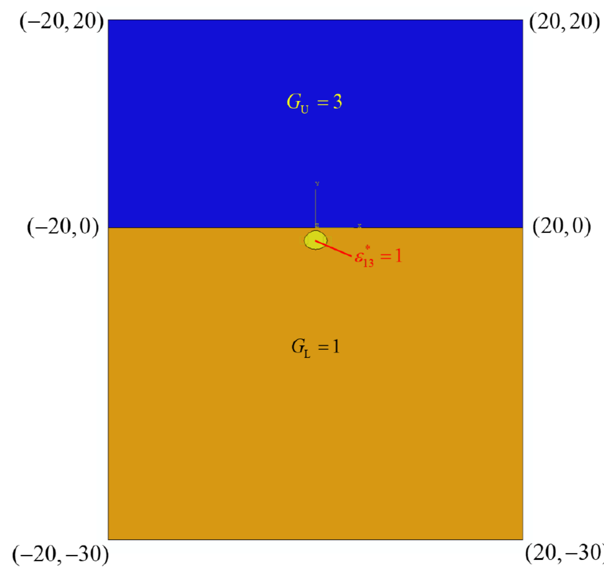


**Figure 6** A bi-material structure containing an inclusion of specific configuration defined by Eq. (60) for finite element simulations.

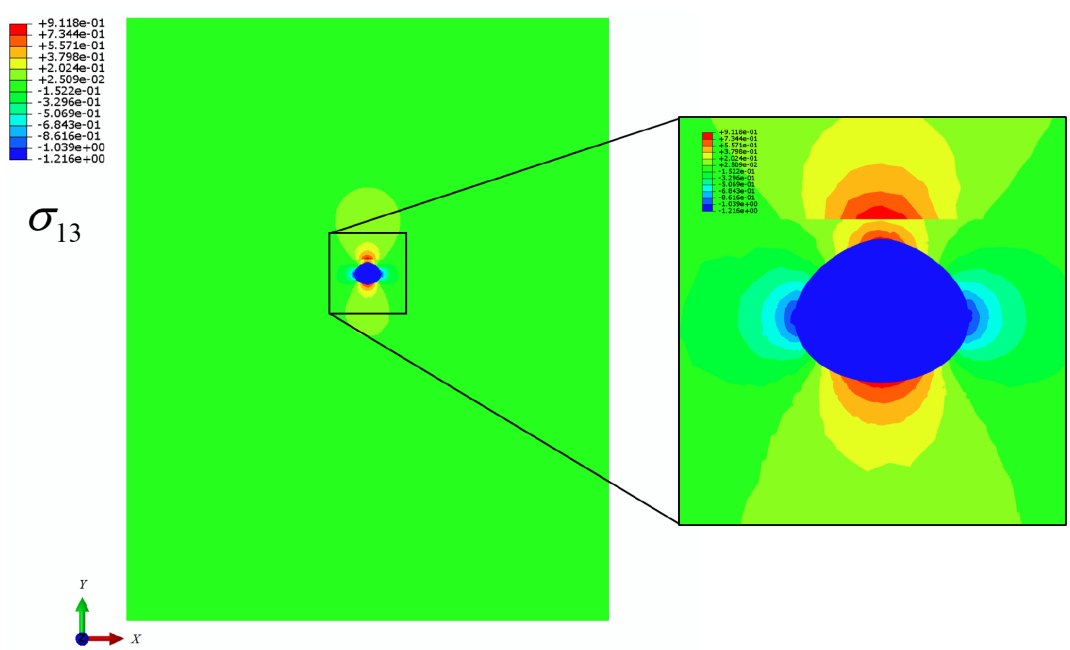


**Figure 7** Stress contour plot for $\sigma_{13}$ in the entire bi-material structure.

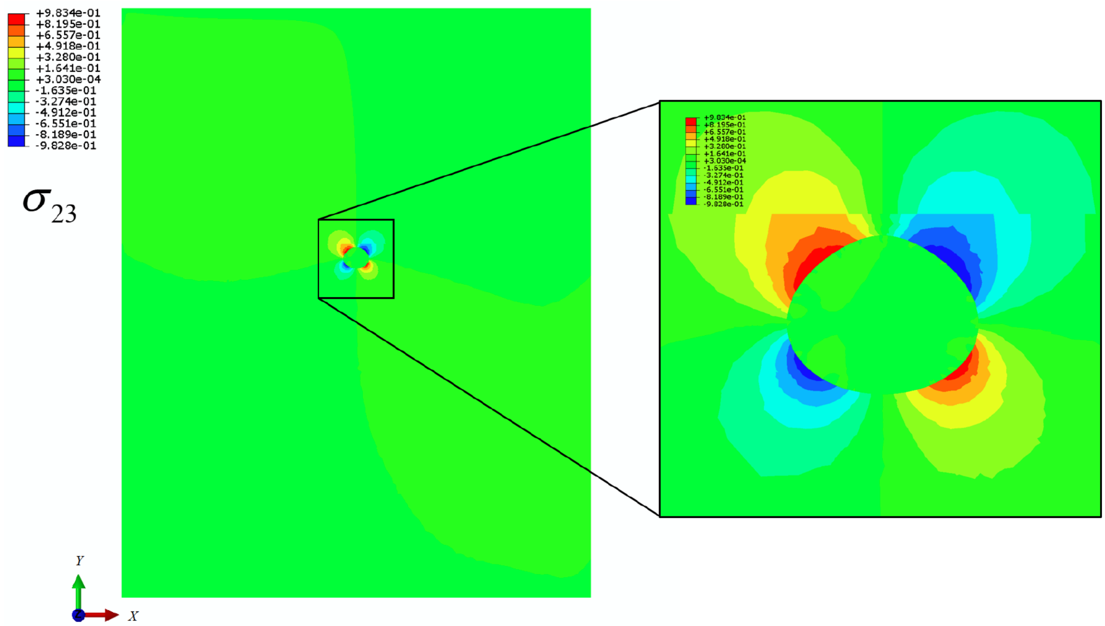


**Figure 8** Stress contour plot for $\sigma_{23}$ in the entire bi-material structure.

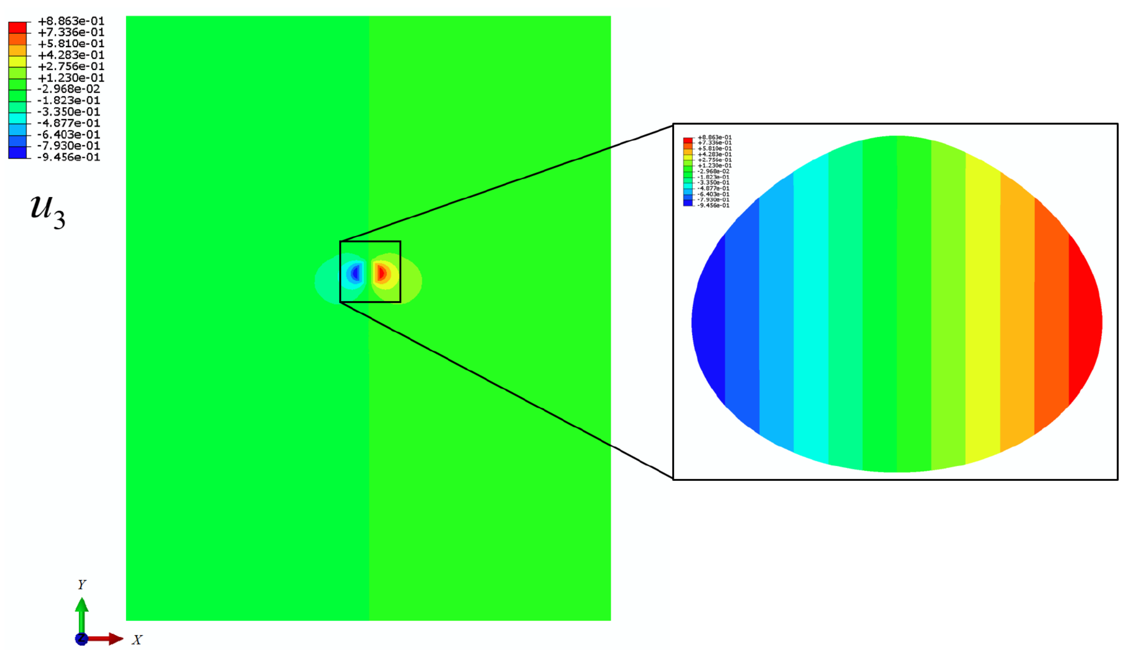


**Figure 9** Displacement contour plot for $u_3$ in the entire bi-material structure.

structure are illustrated in Figs. 7-9, respectively. As displayed from Figs. 7 and 8, the stress inside the inclusion defined by Eq. (60) is indeed quite uniform with its $\sigma_{13}$-component being around $-1.21$ and its $\sigma_{23}$-component being at the level $10^{-4}$ (both are consistent with the theoretical results given in Eq. (61), verifying the accuracy of our algorithm). In addition, the contour plot for the displacement inside the inclusion in Fig. 9 exhibits a linear distribution in the $x_1$-direction, confirming that the stress in the inclusion is uniform with its $\sigma_{23}$-component approaching zero.

## 5. Conclusions

We consider the anti-plane shear deformation of an inclusion with a uniform eigenstrain when it is embedded in an infinite bi-material composite which incorporates two elastic half-planes (the upper one and the lower one) and an infinitely long straight interface between them. The inclusion is contained in the lower half-plane and has the same shear modulus as that of the lower half-plane. Distinct from the conventional forward problem in which one focuses on the determination of the eigenstrain-caused stress field in the entire composite for a given geometry of the inclusion, the current problem is defined as an inverse problem in which we aim at discovering the configuration of the inclusion that makes the eigenstrain-induced stress inside the inclusion uniform.

Instead of any purely numerical optimization algorithm, two analytic methods are used to examine such an inverse problem. One is based on the analytic continuation and the existence theorem of a holomorphic function involving specific-form boundary values, while the other concerns the Green's function for a concentrated force acting on a similar bi-material composite but composed of two complete half-planes (involving no inclusion). As a consequence of employing either of the two methods, we obtain an exact integral equation of the boundary curve of the inclusion which is sufficiently and necessarily responsible for the uniformity of the eigenstrain-induced stress within the inclusion. By introducing a polynomial mapping function with a set of unknown coefficients to parameterize the shape of the inclusion, we then transform the integral equation into a group of nonlinear algebraic equations with respect to the unknown coefficients with the aid of the Faber polynomials and Faber series for a finite simply-connected domain. These equations are solved numerically by classical iterative algorithms, and some representative results of the shape of the inclusion corresponding to a uniform internal stress are analyzed and illustrated. Among others, the phenomena observed from the numerical results are summarized as follows:

(1) For the case in which the plane of the applied shear eigenstrain is parallel to the interface between the two half-planes, the increasing stiffness of the interface (relative to the shear modulus of the inclusion) raises its attraction to the inclusion possessing a constant stress, leading to that a sharp corner oriented to the interface may appear on the boundary of the inclusion as the interface becomes stiffer. In contrast, for the case in which the plane of the applied shear eigenstrain is perpendicular to the interface, the increasing stiffness of the interface decreases its attraction or equivalently increases its repulsion to the inclusion with a constant stress, resulting in that the boundary of the inclusion tends to be even as the interface turns stiffer.

(2) When two eigenstrains of the same magnitude, whose planes are respectively parallel and perpendicular to the interface between the two half-planes, are applied simultaneously to the inclusion in the design of a constant internal stress inside it, the varying stiffness of the interface has only a minor influence on the distance between the inclusion and the interface, but has a significant influence on the orientation of the configuration of the inclusion.

***Conflict of interest*** *On behalf of all authors, the corresponding author states that there is no conflict of interest.*

***Author contributions*** ***Ming Dai:*** *Conceptualization, Formal analysis, Investigation, Methodology, Writing – original draft.* ***Cun-Fa Gao:*** *Writing – review & editing.*

***Acknowledgements*** *This work was supported by the National Natural Science Foundation of China (Grant No. 11902147), and the Natural Science Foundation of Jiangsu Province (Grant No. BK20190393). Special appreciation goes to Mr. Sun Molin for his help in preparing the numerical simulations. Thanks also go to three anonymous reviewers whose comments have led to improvements in the manuscript.*

1 K. Ghosh, and O. Lopez-Pamies, Elastomers filled with liquid inclusions: Theory, numerical implementation, and some basic results, J. Mech. Phys. Solids **166**, 104930 (2022).
2 C. Q. Ru, A simple model for elastic wave propagation in hard sphere-filled random composites, J. Acoust. Soc. Am. **152**, 1595 (2022).
3 C. Chen, L. Wu, J. Fu, C. Xin, W. Liu, and H. Duan, A micromechanical scheme with nonlinear concentration functions by physics-guided neural network, J. Mech. Phys. Solids **188**, 105681 (2024).
4 Q. Zhang, Y. Shi, and C. Gao, The determination of the curing induced, nonlinear elastic field of an inclusion in photo-cured materials, Int. J. Solids Struct. **302**, 112978 (2024).
5 H. Li, and Y. Li, An extended Flaherty-Keller formula for an elastic composite with densely packed convex inclusions, Calc. Var. **61**, 90 (2022).
6 T. Yuan, and L. Liu, Polynomial inclusions: Definitions, applications, and open problems, J. Mech. Phys. Solids **181**, 105440 (2023).
7 D. Choi, and M. Lim, Construction of inclusions with vanishing generalized polarization tensors by imperfect interfaces, Stud. Appl. Math. **152**, 673 (2024).
8 L. P. Liu, Hashin-Shtrikman bounds and their attainability for multi-phase composites, Proc. R. Soc. A **466**, 3693 (2010).
9 L. Silvestre, A characterization of optimal two-phase multifunctional composite designs, Proc. R. Soc. A **463**, 2543 (2007).
10 S. Vigdergauz, Two-dimensional grained composites of minimum stress concentration, Int. J. Solids Struct. **34**, 661 (1997).
11 L. Liu, R. James, and P. Leo, New extremal inclusions and their applications to two-phase composites, arXiv: 2107.04088.
12 G. P. Cherepanov, Inverse problem of the plane theory of elasticity, J. Appl. Math. Mech. (Prikladnaya Matematika of Mechanika) **38**, 963 (1974).
13 L. T. Wheeler, and I. A. Kunin, On voids of minimum stress concentration, Int. J. Solids Struct. **18**, 85 (1982).
14 J. S. Marshall, On sets of multiple equally strong holes in an infinite elastic plate: parameterization and existence, SIAM J. Appl. Math. **79**, 2288 (2019).
15 G. S. Bjorkman Jr., and R. Richards Jr., Harmonic holes—An inverse problem in elasticity, J. Appl. Mech. **43**, 414 (1976).
16 M. Dai, Some rigorous results for harmonic holes with surface tension, Int. J. Solids Struct. **303**, 113012 (2024).
17 N. J. Hardiman, Elliptic elastic inclusion in an infinite elastic plate, Q. J. Mech. Appl. Math. **7**, 226 (1954).
18 S. X. Gong, and S. A. Meguid, A general treatment of the elastic field of an elliptical inhomogeneity under antiplane shear, J. Appl. Mech. **59**, S131 (1992).
19 C. Q. Ru, and P. Schiavone, On the elliptic inclusion in anti-plane shear, Math. Mech. Solids **1**, 327 (1996).
20 G. P. Sendeckyj, Elastic inclusion problems in plane elastostatics, Int. J. Solids Struct. **6**, 1535 (1970).
21 J. D. Eshelby, The determination of the elastic field of an ellipsoidal inclusion and related problems, Proc. R. Soc. A **241**, 376 (1957).
22 L. P. Liu, Solutions to the Eshelby conjectures, Proc. R. Soc. A **464**, 573 (2008).
23 H. Kang, and G. W. Milton, Solutions to the Pólya-Szegö conjecture and the weak Eshelby conjecture, Arch. Ration. Mech. Anal. **188**, 93 (2008).

24 H. Ammari, Y. Capdeboscq, H. Kang, H. Lee, G. W. Milton, and H. Zribi, Progress on the strong Eshelby's conjecture and extremal structures for the elastic moment tensor, J. de Mathématiques Pures Appliquées **94**, 93 (2010).
25 T. Yuan, K. Huang, and J. Wang, A constrained proof of the strong version of the Eshelby conjecture for three-dimensional isotropic media, Acta Mech. Sin. **39**, 422064 (2023).
26 T. Yuan, K. Huang, and J. Wang, Solutions to the generalized Eshelby conjecture for anisotropic media: Proofs of the weak version and counter-examples to the high-order and the strong versions, J. Mech. Phys. Solids **158**, 104648 (2022).
27 X. Wang, L. Chen, and P. Schiavone, Uniform stress field inside an anisotropic non-elliptical inhomogeneity interacting with a screw dislocation, Eur. J. Mech.-A Solids **70**, 1 (2018).
28 X. Wang, L. Chen, and P. Schiavone, Uniformity of stresses inside a non-elliptical inhomogeneity interacting with a mode III crack, Proc. R. Soc. A **474**, 20180304 (2018).
29 M. Dai, P. Schiavone, and C. F. Gao, Nano-inclusion with uniform internal strain induced by a screw dislocation, Arch. Mech. **68**, 243 (2016).
30 X. Wang, P. Yang, and P. Schiavone, Uniform stresses inside a non-elliptical inhomogeneity and a nearby half-plane with locally wavy interface, Z. Angew. Math. Phys. **71**, 58 (2020).
31 H. Kang, E. Kim, and G. W. Milton, Inclusion pairs satisfying Eshelby's uniformity property, SIAM J. Appl. Math. **69**, 577 (2008).
32 X. Wang, Uniform fields inside two non-elliptical inclusions, Math. Mech. Solids **17**, 736 (2012).
33 M. Dai, C. F. Gao, and C. Q. Ru, Uniform stress fields inside multiple inclusions in an elastic infinite plane under plane deformation, Proc. R. Soc. A **471**, 20140933 (2015).
34 M. Dai, C. Q. Ru, and C. F. Gao, Uniform strain fields inside multiple inclusions in an elastic infinite plane under anti-plane shear, Math. Mech. Solids **22**, 114 (2017).
35 Y. A. Antipov, Method of automorphic functions for an inverse problem of antiplane elasticity, Q. J. Mech. Appl. Math. **72**, 213 (2019).
36 M. Dai, C. Q. Ru, and C. F. Gao, Non-elliptical inclusions that achieve uniform internal strain fields in an elastic half-plane, Acta Mech. **226**, 3845 (2015).
37 Y. A. Antipov, Riemann-Hilbert problem on a hyperelliptic surface and uniformly stressed inclusions embedded into a half-plane subjected to antiplane strain, Proc. R. Soc. A **477**, 20210350 (2021).
38 X. Wang, L. Chen, and P. Schiavone, Uniformity of stresses inside a non-elliptical inhomogeneity interacting with a circular Eshelby inclusion in anti-plane shear, Arch. Appl. Mech. **88**, 1759 (2018).
39 X. Wang, P. Yang, and P. Schiavone, A circular Eshelby inclusion with linear eigenstrains interacting with a coated non-parabolic inhomogeneity with internal uniform anti-plane stresses, Eur. J. Mech.-A Solids **87**, 104219 (2021).
40 X. Wang, and P. Schiavone, A non-circular inhomogeneity near a non-elliptical inhomogeneity designed to admit an internal uniform hydrostatic stress field, Mech. Mater. **162**, 104072 (2021).
41 J. Dundurs, Elastic interaction of dislocations with inhomogeneities, in: Mura, T Mathematical Theory of Dislocations (ASME, New York, 1969). pp. 70-115.
42 N. I. Muskhelishvili, Some Basic Problems of the Mathematical Theory of Elasticity (Springer, Dordrecht, 1975).
43 G. Faber, Über polynomische Entwickelungen, Math. Ann. **57**, 389 (1903).

# 均匀应力夹杂在双材料界面附近的形状演化: 反平面变形

戴明, 高存法

**摘要** 在二维线弹性力学框架下, 对于均质无限大基体中的椭圆夹杂, 当夹杂受到均匀的本征应变时, 夹杂内部则会产生均匀的应力. 在此背景下, 我们拟探讨这样一个问题: 当基体中某个初始形状为椭圆的夹杂遇到材料界面时, 其形状应如何演化才能继续保证内部应力的均匀性呢? 为此, 我们在反平面变形下考虑一个含有夹杂的双材料结构, 该结构由两个无限大半平面构成, 夹杂受到均匀的本征应变, 其形状作为待求解的未知数使得夹杂内部获得均匀应力. 然而, 和绝大多数拓扑优化算法不同的是, 本文侧重通过严密的理论分析直接获得夹杂形状应满足的方程, 该方程被证明是一个关于夹杂边界曲线的非线性积分方程. 我们借助一些解析分析手段最终获得了该方程的半解析解. 通过具体的算例, 我们展示了一系列能够确保内部均匀应力的夹杂形状, 并研究了夹杂形状随双材料界面刚度的演化规律.